Industrial symbiosis of anaerobic digestion and pyrolysis: Performances and agricultural interest of coupling biochar and liquid digestate

Saida Tayibi, Florian Monlau, Frederic Marias, Nicolas Thevenin, Raquel Jimenez, Abdallah Oukarroum, Adil Alboulkas, Youssef Zeroual, Abdellatif Barakat

Industrial symbiosis of anaerobic digestion and pyrolysis: performances and agricultural interest of coupling biochar and liquid digestate

Saida Tayibi[1, 2, 3, 4], Florian Monlau[3*], Frederic Marias[5], Nicolas Thevenin[6], Raquel Jimenez[3], Abdallah Oukarroum[2], Adil Alboulkas[1,7], Youssef Zeroual[8], and Abdellatif Barakat[1,2*]

[1]IATE, University of Montpellier, INRAE, Agro Institut of Montpelier, Montpellier, France
[2] Mohammed VI Polytechnic University (UM6P), Ben Guerir, Morocco
[3]APESA, Pôle Valorisation, Cap Ecologia, Lescar, France
[4] LIMAT, Faculté des Sciences Ben M'Sik, Université Hassan II de Casablanca, Morocco
[5] Laboratoire de Thermique Energétique et Procédés – IPRA, EA1932, Université de Pau et des Pays de l'Adour/E2S, UPPA, 64000 Pau, France
[6] RITTMO Agroenvironnement-ZA Biopôle – 37 rue de Herrlisheim– CS 800 23 – 68025 COLMAR CEDEX, France
[7] Laboratoire des procédés chimiques et matériaux appliqués (LPCMA), Faculté polydisciplinaire de Béni-Mellal, Université Sultan Moulay Slimane, BP 592, 23000 Béni-Mellal, Morocco
[8] Situation Innovation, OCP Group, Complexe industriel Jorf Lasfar, El Jadida, Morocco

[*]Corresponding author: Florian Monlau; Email: florian.monlau@apesa.fr; abdellatif.barakat@inrae.fr Tel: +33688491845

GRAPHICAL ABSTRACT

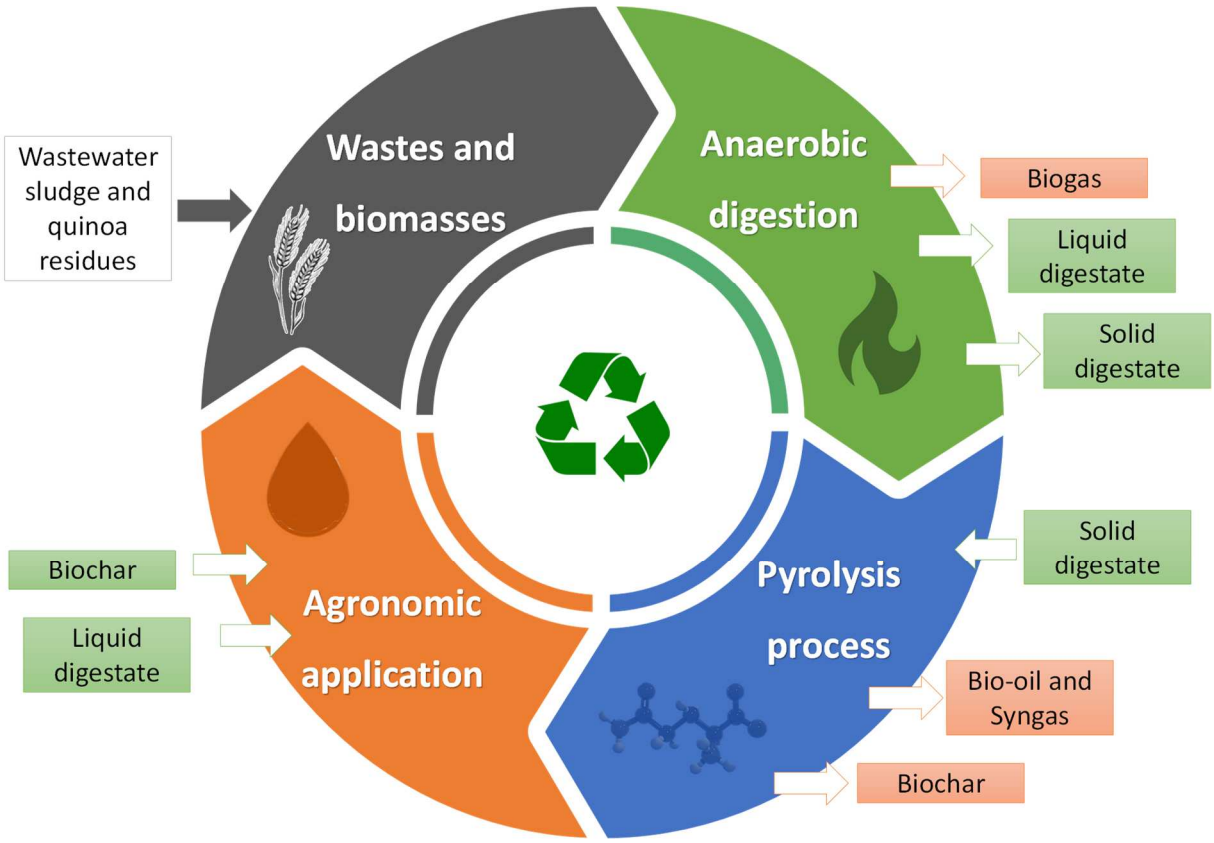

Keywords: Anaerobic digestion, biochar, biogas, bio-oil, mineralization, plant growth tests, syngas

Abbreviations:

AD: Anaerobic digestion

B25: Biochar at 25 tons/ha

B50: Biochar at 50 tons/ha

BMP: Biochemical Methane Potential

CHP: Cogeneration Heat and Power

COD: Chemical Oxygen Demand

CSTR: Continuous Stirred Tank Reactor

DM: Dry Matter

EBC: European Biochar Certificate

IBI: International Biochar Initiative

IF: Industrial Fertilizer (DAP and ammonium nitrate)

LD: Liquid Digestate

VS: Volatile Solid

ABSTRACT

The sustainability of the anaerobic digestion industry is closely related to proper digestate disposal. In this study, an innovative cascading biorefinery concept coupling anaerobic digestion and subsequent pyrolysis of the digestate was investigated with the aim of enhancing the energy recovery and improving the fertilizers from organic wastes. Continuous anaerobic co-digestion of quinoa residues with wastewater sludge (45/55% VS) exhibited good stability and a methane production of 219 NL CH_4/ kg VS. Subsequent pyrolysis of the solid digestate was carried out (at 500 °C, 1 h, and 10 °C/min), resulting in a products distribution of 40 wt% biochar, 36 wt% bio-oil, and 24 wt% syngas. The organic phase (OP) of bio-oil and syngas exhibited higher and lower heating values of 34 MJ/kg and 11.8 MJ/Nm^3, respectively. The potential synergy of coupling biochar with liquid digestate (LD)

for agronomic purposes was investigated. Interestingly, coupling LD (at 170 kgN/ha) with biochar (at 25 tons/ha) improved the growth of tomato plants up to 25% compared to LD application alone. In parallel, co-application of biochar with LD significantly increased the ammonia volatilization (by 64%) compared to LD application alone, although their simultaneous use did not impact the C and N mineralization rates.

1. Introduction

The increase in the world's population is creating environmental issues such as over-exploitation of fossil fuels and the accumulation of wastes. In recent decades, the scientific community has increasingly engaged in the development of processes that optimize the recovery and use of organic wastes (biowastes, agricultural wastes, agro-industrial wastes, urban wastes, etc.) in a diverse range of products according to the concept of environmental biorefineries (Demichelis et al., 2020; Monlau et al., 2015a). Morocco has rapidly transformed into a largely urban society over the past decade, with approximately 60% of its citizens now living in cities and urban areas due to a trend of rural migration to coastal centers. The high population growth rate in urban agglomerations in recent years has been accompanied by environmental problems such as an increase in wastes and effluents (Alhamed et al., 2018; Belloulid et al., 2017). Morocco has achieved significant improvement in the wastewater sector in the past ten years, and 123 wastewater treatment plants (WWTP) have been built, increasing the treatment capacity to 900 million m^3 per year (Alhamed et al., 2018). In 2015, the potential production of sludge in Morocco at the level of WWTP was estimated to 155,450 tons of dry matter (Belloulid et al., 2017).

Anaerobic digestion (AD) is a well-known process that has been used for many decades to treat organic wastes, such as wastewater sludges (Sawatdeenarunat et al., 2016). This process transforms organic matter in the absence of oxygen into biogas (a mixture of CH_4 and CO_2) and an undegraded residue called digestate (Monlau et al., 2015b). Biogas is a source of

energy that is generally used to generate heat and electricity through cogeneration and a heat power system or it can be injected into the natural gas grid after an upgrading process (Roubaud and Favrat, 2005). Nonetheless, mono-AD of organic wastes is limited by the need to maintain an optimal C/N ratio between 15 and 30 (Chandra et al., 2012), which can lead to instability and decreased performance (Sawatdeenarunat et al., 2016). Anaerobic co-digestion with lignocellulosic biomass is a promising technology to improve digester performance with wastewater sludge by improving the C/N ratio (Giuliano et al., 2013; Zhao et al., 2018). Despite the potential of co-digestion technology, lignocellulosic biomass as a co-substrate can lead to a significant increase in the volume of digestate, thus requiring a final elimination/valorization step (González et al., 2020). Generally, the anaerobic digestate is separated into a liquid fraction (rich in nutrients, especially N and K) and a solid fraction rich in P and fibers that are mostly separated by a filter press, centrifuge, or a vibrating sieve (Akhiar et al., 2017).

The cascading biomass valorization approach by coupling two or three processes has become a new strategy to achieve the "zero waste" goal at the industrial scale. Recently, the coupling of anaerobic digestion (AD) and pyrolysis processes through the pyrolysis of solid digestate has been considered as a solution to the challenge of AD digestate management and a way to increase the sustainability of the entire process by the production of a higher amount of biofuels (syngas and bio-oil) (Fabbri and Torri, 2016; Ghysels et al., 2020; González et al., 2020; Pecchi and Baratieri, 2019). Pyrolysis is a thermochemical process in which biomass is thermally degraded under an inert or a very low stoichiometric oxygen atmosphere (Tripathi et al., 2016), yielding three products: syngas (mainly CO_2, H_2, and CO), bio-oil (composed of an organic and an aqueous phases), and biochar (Monlau et al., 2015). Syngas can be converted into heat or heat/electricity (combined heat and power, CHP) alone or mixed with biogas in boilers and engines (Seyedi et al., 2019). The organic phase of bio-oil can be used as

104 a fuel, or it can be added to petroleum refinery products or upgraded by catalysts to produce
105 premium-grade refined fuels, or it may have use as building blocks (Pütün et al., 2005)
106 whereas the aqueous phase can be recirculated as feedstock for the AD process (Torri and
107 Fabbri, 2014). The energetic interest of coupling AD and pyrolysis compared to stand-alone
108 AD has been demonstrated previously (Ghysels et al., 2020; Monlau et al., 2015b). In parallel,
109 González-Arias et al. (2019) demonstrated that the combined approach of pyrolysis and
110 digestion solves the digestate disposal problem by generating biochar. Indeed, biochar, which
111 is the carbonaceous material obtained from pyrolysis, has several advantages (stable C,
112 hygienization, water retention, etc.) and it can be used in several environmental applications
113 (Abdeljaoued et al., 2020). For instance, biochar has gained much attention in recent decades
114 due to its potential to enhance soil quality and soil preservation, as well as mitigation of
115 climate change by carbon sequestration (Fernández et al., 2014; Semida et al., 2019).

116 Nonetheless, although coupling AD and pyrolysis has been well described and discussed in
117 the literature from an energetic point of view, less information is available regarding the use
118 of biochar derived from solid digestate for agronomic applications used alone or in
119 combination with liquid digestate (Glaser et al., 2015; Opatokun et al., 2017; Tayibi et al.,
120 2021). Ronga et al. (2020) assessed the effect of combining biochar (from pine wood chips)
121 with LD (from AD of a mixture of maize silage, triticale silage, cow slurry, and grape stalks)
122 on the fruit yield of tomatoes produced by organic farming. The results demonstrated that
123 tomato plants fertilized with LD and biochar achieved a maximum yield of 72 tons/ha, while
124 the lowest production of 47 tons/ha was recorded with unfertilized plants (Ronga et al., 2020).
125 Similarly, Tayibi et al., (2020a) investigated the coupling of LD with biochar (produced from
126 the solid digestate fraction) for agronomic applications on nutrient leaching and wheat
127 growth. Interestingly, the addition of biochar increased the cumulative leaching of all
128 nutrients, except nitrate, with a significant decrease of 82% at 50 tons/ha, compared to soil

treated only with LD alone. In parallel, co-application of biochar and LD improved the aerial dry biomass production of wheat (up to 27.5%) compared to soil treated only with LD. Nonetheless, there is still little information available regarding the coupling of LD and biochar, not only in terms of crop yields but also on changes in the physicochemical properties of soil. The present study, therefore, evaluated the following:

- The performance of a continuous stirred reactor (CSTR) at a pilot scale for co-digestion of quinoa residues and wastewater sludge;
- The pyrolysis products (biochar, bio-oil, and syngas) from a solid digestate at 500 °C, 1 h, and 10 °C/min;
- Characterization of the syngas, bio-oil, and biochar by evaluation of the content of the inorganic elements contained in the biochar with the range suggested by the International Biochar Initiative (IBI) and the European Biochar Certificate (EBC).
- The phytotoxicity (germination index) of co-application of biochar (25 tons/ha and 50 tons/ha) and LD (170 kg N /ha) on tomato plants;
- The effect of co-application of biochar (25 tons/ha) and liquid digestate (170 kg N/ha) on microbial respiration (CO_2), the mineralization of nitrogen, and the volatilization of ammonia.

2. Materials and Methods

2.1. Feedstocks, inoculum, and soil properties

Two different residues were used for the anaerobic digestion tests: wastewater sludge and quinoa residues. The wastewater sludge was collected from a WWTP located in Lescar (France) and stored at -16 °C. Quinoa residues were collected from a private farm located in Benguerir (Morocco), the residues were dried at 40 °C for three days and crushed twice using an electric vegetable mill (Ge250, Stihl Viking®, Germany). The inoculum used for the biochemical methane potential (BMP) tests and for the semi-continuous assays was an

internal mesophilic inoculum produced at the APESA center and fed with a mixture of wastewater sludge and grass. For the agronomic tests, an agricultural soil sampled at the surface (0-25 cm) was collected at the INRAE site in Mauguio (15.8 km from Montpellier, France). The soil was air-dried and passed through a 2-mm sieve to remove large fragments. The main characteristics of the soil were (per thousand parts of raw material): 210 parts clay (< 2μm), 93 parts fine silt (2 to 20 μm), 208 parts coarse silt (20 to 50 μm), 196 parts fine sand (50 to 200 μm), and 302 parts coarse sands (200 to 2,000 μm). The soil was classified as a clay loamy soil. Some of the other characteristics of the soil were a pH of 7.4 ± 0.1 (water), 1.9 ± 0.2% organic matter, a C/N ratio of 10.1, a total nitrogen (TN) content of 0.1 wt%, 0.1 ± 0.02 g/kg phosphorus (P_2O_5), 0.4 g/kg potassium (K_2O), and a 9.9 ± 1.0 cmol (+)/kg cation exchange capacity (CEC). Two commercial fertilizers were used: DAP $(NH_4)_2HPO_4$, characterized by 18 wt% N-NH_4 and 46 wt% P-P_2O_5, provided by the Cherifian Office for Phosphates (OCP) company and complemented with ammonium nitrate (NH_4NO_3) (99%), from Sigma-Aldrich®, to obtain a ratio of 170 kg N/ha.

2.2. Anaerobic digestion (AD) process

The BMP tests were performed under anaerobic mesophilic conditions (35 ± 2 °C, pH = 7) and in duplicate with a working volume of 500 mL at a substrate inoculum (S/I) ratio of 0.35 according the recommendations made in the European Interlaboratory study (Hafner et al., 2020). A blank control (only the inoculum) was carried out in parallel with the other biomasses that were tested (wastewater sludge and quinoa residues) to subtract the amount of biogas generated by just the inoculum. Once the bottle was prepared, it was purged with nitrogen gas (N_2) to maintain anaerobic conditions. The bottles were then sealed and placed in an oven at 35 ± 2 °C to maintain mesophilic conditions. The biogas production was monitored daily by pressure measurements using a manometer with an LC display (Testo 502, TESTOON, France). The composition of the biogas (H_2, O_2, N_2, CH_4, CO_2, and H_2S) was

181 determined using a micro gas chromatograph (490, Agilent Technology, USA). The first
182 column (Molsieve 5Å PLOT) was used at 110 °C to separate the O_2, N_2, and CH_4, and the
183 second column (HayeSep A) was used at 70 °C to separate the CO_2 from the other gases. The
184 injector and the detector temperatures were 110 °C and 55 °C, respectively. Detection of the
185 gaseous compounds was performed using a thermal conductivity detector. The calibration was
186 performed with two standard gases composed of either 9.5% CO_2, 0.5% O_2, 81% N_2, and 10%
187 CH_4 or 35% CO_2, 5% O_2, 20% N_2, and 40% CH_4 (Air Liquide®). All of the results are
188 presented under standardized conditions of temperature and pressure (Patm, 0 °C). After
189 determination of the BMP of the substrates (quinoa residues and wastewater sludge), a
190 continuously stirred tank reactor (CSTR) assay was set up with a total working volume of 20
191 L under mesophilic conditions (35 ± 2 °C) and homogeneity was maintained using a
192 continuous agitation system. The reactor was initially supplied with mesophilic inoculum as
193 previously described. The feedstock input and the discharge digestate were performed
194 manually once a day (5 days per week). The feedstock mixture was composed of 42.5% VS
195 wastewater sludge and 57.5% VS quinoa residues. The organic load rate and the hydraulic
196 retention time were set at 2.06 g VS/m^3 day and 41 days, respectively. The CSTR was
197 monitored by measurement of the pH and the temperature on a daily basis, the FOS/TAC
198 (Free Organic Acids / Total Inorganic Carbonate) ratio twice a week, and the volatile fatty
199 acids (VFAs) as well as the ammonium concentration once a week. Details for all the
200 experimental protocols are provided in the previous section. Measurement of the Dry Matter
201 (DM) and the Volatile Solid (VS) contents of the digestate was carried out every weekend.
202 The biogas produced was recorded every day by a PC system connected to a Ritter volumetric
203 counter cell. The biogas was collected in a gas pocket directly connected to the gas meter; the
204 analysis of the biogas was carried out 5 days/week using micro gas chromatography (490,
205 Agilent Technology, USA) as previously described. At the end of the process, a solid-liquid

206 separation was carried out using a wine press. A mass balance of the chemical oxygen
207 demand (COD) was also carried out at the end of the process. To assess the mass balance, it
208 was assumed that 350 NL CH_4 can be produced per kg of COD. The COD of the solid
209 digestate was assessed by a modified protocol using a double acid hydrolysis of biomasses as
210 described by Cazaudehore et al. (2019). The supernatant liquids from the solid fraction and
211 the LD were analyzed for COD using commercial kits (Spectroquant 14,155, Merck,
212 Germany). The concentrations ranged from 500 to 10,000 mg COD/L. The tubes were then
213 heated to 148 °C in a preheated thermoreactor for 120 min. Finally, the COD was measured
214 by an automatic spectrophotometer (photoLab® S6, WTW, Germany).

215 **2.3 Pyrolysis test of the solid digestate**

216 The dried solid digestate sample (approximately 300 g) was subjected to pyrolysis in a steel
217 reactor. Before the pyrolysis, the basket of feedstock and the furnace were purged with N_2 for
218 30 min to ensure an oxygen-free environment. The experiments were then carried out in
219 duplicate at 500 °C with a heating rate of 10 °C/min, for 1 hour at high temperature. The
220 collected pyrolysis products were biochar, bio-oil (condensable gas), and syngas (non-
221 condensable gas). The furnace was then cooled to 25 °C under nitrogen flow and the biochar
222 and bio-oil were collected and weighed. The syngas (hydrogen, oxygen, nitrogen, carbon
223 monoxide, and dioxide, methane, ethane, and ethylene) was quantified using a micro-
224 chromatography device (Varian CP-4900, Agilent, Germany). The first column (CP-Sil CB)
225 was operated at 37 °C to separate the H_2 and the O_2, while the second column (Molsieve 5Å
226 PLO) was operated at 37 °C to separate the N_2, CO, and CH_4, and the third column (HayeSep
227 A) was operated at 35 °C to separate the CO_2, C_2H_2, C_2H_4, and C_2H_6. The gaseous compounds
228 were detected by a thermal conductivity detector. The injector and the detector temperatures
229 were 50 °C and 55 °C, respectively. The analyses of the syngas were carried out every 5
230 minutes during the pyrolysis reaction using the micro-GC. The mass of the produced syngas

M_{Syngas} (g) was determined by the difference between the output and input gas flow during the pyrolysis process using an acquisition system linked to two flowmeters measuring the input (flowmeter BROOKS) and the output (flowmeter M.M.T). Equation (1) was used to calculate the mass of the syngas, as described below:

$$M_{Syngas}(g) = \sum \left(output\ flow\ (g/min) - input\ flow\ (g/min)\right)/122 \quad (1)$$

where 122 is the number of acquisitions per min.

The biochar, bio-oil, and syngas product yield percentages were calculated as follows:

$$Biochar\ (wt\%) = M_{Biochar}(g)/M_{Solid\ digestate}\ (g) \times 100 \quad (2)$$

$$Bio-oil\ (wt\%) = M_{Bio-oil}(g)/M_{Solid\ digestate}(g) \times 100 \quad (3)$$

$$Syngas\ (wt\%) = M_{Syngas}(g)/M_{Solid\ digestate}(g) \times 100 \quad (4)$$

where $M_{Biochar}$, $M_{Bio\text{-}oil,}$ and M_{Syngas} represent the biochar, bio-oil, and syngas masses produced during the pyrolysis, and $M_{solid\ digestate}$ represents the mass of the solid digestate.

The losses during pyrolysis (approximately 6%) were considered to be the bio-oil trapped in the walls of the cooling system, and they were taken into account in the bio-oil calculation.

The bio-oil obtained in this work was separated into two different phases: an organic phase and an aqueous phase obtained by decantation using dichloromethane (99.8%, from Sigma-Aldrich®) as the organic solvent. The weight and the yield were measured after decantation. Anhydrous Na_2SO_4 was added to the solvent mixture/organic phase to remove residual water. The solvent was then evaporated using a rotary evaporator, the organic phase of bio-oil was weighed, and its yield was measured.

The average lower heating value (LHV) of the syngas was calculated based on Equation (5) (Lv et al., 2004), assuming that the N_2 had been separated from the produced syngas. The

predictive higher heating value (HHV) (MJ/kg) of the organic phase of the bio-oil was calculated using ultimate analysis in Equation (6) (Troy et al., 2013) as follows:

$$LHV(MJ\ /Nm^3) = [30 \times v/v\%\ CO + 25.7 \times v/v\%\ H_2 + 85.4\ \times v/v\%\ CH_4 + 151.3 \times v/v\%\ (C_2H_4 + C_2H_6)] \times 0.42] \quad (5)$$

$$HHV\ (MJ/\ kg) = [3.55 \times C^2 - 232 \times C - 2230 \times H + 51.2 \times (C \times H) + 131 \times N + 20,600]/1000 \quad (6)$$

2.4 Analytical methods

2.4.1. Physicochemical analysis

The Dry Matter (DM) and Volatile Solids (VS) contents in the organic wastes and the co-products were determined according to the protocol outlined by the American Public Health Association (APHA, 2005). The pH of the digestate was determined using a WTW 340i reference pH meter. Ammonium (NH_4^+) was determined using reagent kits (Spectroquant®, Germany) for NH_4^+ by spectrophotometry (photoLab® S6, WTW, Germany). To determine the concentration of the VFAs, the digestate was centrifuged for 20 minutes at 9,600 rpm using a centrifuge system (Hettich Zentrifugen, Rotanta 460) to recover the liquid fraction. An internal standard solution was prepared from 1 g of ethyl-2-butyric acid diluted in 1 L of water acidified with 2.5% phosphoric acid. A 1 mL aliquot of internal standard solution was then added to 2 mL of the liquid sample. The mixture was filtered using a 0.2-µm nylon filter attached to a syringe. The filtered liquid was introduced into a vial for analysis by a gas chromatography system (GC-7890B) coupled to a flame ionization detector (FID). The FOS/TAC (Free Organic Acids / Total Inorganic Carbonate) ratio, which corresponds to the total acid and buffer capacity levels, was determined by acidification of the sample prepared as 2 g of digestate diluted in 50 mL of deionized water under magnetic agitation with sulfuric acid (0.1 N) from a graduated burette. A first acidification to a pH of 5.1 determines the buffer capacity of the medium. A second acidification to a pH of 3.5 can quantify the amount of total acids in the medium. The Chemical Oxygen Demand (COD) of the LD was analyzed

using commercial kits (Spectroquant®, Merck, Germany). A 1 mL aliquot of centrifuged LD was placed in the commercial tubes. The tubes were then heated to 148 °C in a preheated thermoreactor for 120 min. Finally, the COD was measured by an automatic spectrophotometer (photoLab® S6, WTW, Germany). The theoretical COD of the feedstocks (wastewater sludge and quinoa residues) and the solid digestate were determined based on CHNS analysis according to the method reported by Wei et al., (2018). For the COD balances and biogas equivalence presented in **Fig. 2**, it was assumed that 1g of COD is equivalent to 1NmL of CH_4 (Im et al., 2020). The total Kjeldahl Nitrogen (TKN) content of the soil and the LD was determined according to the Kjeldahl method (Kjeldahl, 1883) by using a mineralizator (BUCHI digestion unit K-438) and a distillator/titrator (BUCHI K-370). Moreover, the $N\text{-}NH_4^+$ content of the LD was determined by the titrimetric method after distillation using a BUCHI K-370 distillatory (Rodier, 1975).

A thermogravimetric analyzer (TGA 2-LF, Mettler Toledo®, Switzerland) was used to assess the thermal degradation of the solid digestate and the stability of its biochar, as well as to determine the moisture, volatile matter, fixed carbon, and ash contents according to the protocol reported in Tayibi et al., (2020b). The fibers (cellulose, hemicelluloses) and the Klason lignin content of the dry solid digestate were determined using the NREL protocol (Sluiter et al., 2008). Briefly, the Klason lignin content was determined as the weight of the residues retained on a sintered glass crucible filter (Ø=25mm), and the soluble fractions were analyzed by high-pressure liquid chromatography (HPLC) to quantify the monosaccharides content (i.e., glucose, xylose, and arabinose). The HPLC (Alliance® HPLC System**,** Waters**,** USA) analysis was performed using a column (Aminex® HPX-87H, BioRad, France) at 40 °C and 0.3 mL/min of 0.005 M H_2SO_4. All of the measurements were performed in triplicate. The cellulose and the hemicellulose percentages were determined by Equations (7) and (8), respectively.

$$Cellulose(\%) = [(Glucose(g/L) \times V_{tot})/M_{ini}] \times 100/1.11 \quad (7)$$

$$Hemicelluloses\ (\%) = [(Xylose(g/L) + Arabinose(g/L) \times V_{tot})/M_{ini}] \times 100\ /1.13 \quad (8)$$

where V_{tot} and M_{ini} represent the total volume of the hydrolysis medium (0.025 L) and the initial mass of the sample in grams, respectively, while 1.11 represents the conversion factor between glucose and cellulose and 1.13 represents the conversion factor between monomers (xylose and arabinose) and hemicelluloses (Barakat et al., 2015).

The nutrient content (P, K, Mg, S, Ca, and Na) and the minor metallic content (Pb, Cd, Cu, Ni, Hg, Zn, Cr, and As) were determined by inductively coupled plasma mass spectrometry (ICP-MS) (X SERIES 2 ICP-MS, Thermo Fisher Scientific, USA) equipped with a cooled spray chamber, a quadrupole mass spectrometer, and a collision cell. The ICP-MS settings were as follows: a nebulizer flow of 0.82 L/min, an auxiliary flow of 0.80 L/min, a cool flow of 13 L/min, a forward power of 1,400 Watts, and a cell gas He/H flow rate of 0.0045 L/min. For this purpose, microwave-assisted mineralization of the solid digestate and its biochar was performed after the addition of nitric acid (65%) and hydrogen peroxide (30%). The reaction was conducted for 30 min at room temperature, and the mixtures were then placed in the microwave reactor (flexiWAVE, Milestone, USA) and heated for 20 min to reach 210 °C, which was maintained for 20 min and then cooled for 25 min. The obtained solutions were filtered using 0.2-µm filters and then analyzed by ICP-MS. The ultimate analyses (C, H, N, O, and S) of the dry solid digestate, its biochar, and the organic phase of bio-oil and dry tomato plants were determined in duplicate using an elemental analyzer (varioMicro V4.0.2, Elementar®, Germany).

2.5 Agronomic tests

2.5.1. Carbon mineralization test

The effect of biochar (25 tons/ha) on soil CO_2 emission with or without the addition of LD (170 kg N/ha) was explored by a 91-day indoor incubation experiment based on the AFNOR FD U44-163, (2018) standard. The biochar and the liquid digestate (LD) were added and mixed with the soil as follows: soil, soil + biochar (B25), soil + LD + biochar (B25), and soil + LD. Each condition was distributed into cups containing the equivalent of 25g of dry soil. These cups were then placed in hermetically sealed containers in the presence of sodium hydroxide and incubated at 28 °C. The humidity was kept constant throughout the experiment (equivalent to the field water retention capacity of pF 2.8). The carbon mineralized by the sample was measured after 1, 3, 7, 14, 21, 28, 49, 70, and 91 days of incubation by assessment of the C-CO_2 trapped in the sodium hydroxide (NaOH; 0.5 mol/L). This measurement was performed on three repeats. A mixture of sodium carbonate (Na_2CO_3) and sodium hydroxide was assayed. The carbonates were precipitated with an excess of barium chloride ($BaCl_2$; 20 wt%) solution. The sodium hydroxide that remained free was titrated with hydrochloric acid (HCl; 0.1 mol/L). Thymolphthalein (a 0.1% solution in ethanol) was used as the color indicator. The microbial respiration was calculated according to the following Equation (9):

$$Microbial\ repiration\left(\frac{mg(C-CO_2)}{kg\ dry\ soil}\right) = 0.5 \times \lfloor((M_{NaOH}(mol/L) \times Vol._{NaOH}(L)) - (M_{HCl}(mol/L) \times Vol._{HCl\ used}(L))\rfloor \times Mm_C\left(\frac{g}{mol}\right) \times 1000\ /m_{soil}(kg) \quad (9)$$

where, M_{NaOH} and M_{HCl} are the concentrations of the NaOH and the HCl solutions used in *mol/L*, respectively, $Vol._{NaOH}$ is the volume of the NaOH solution, $Vol._{HCl}$ is the volume of HCl used in the titration (L), Mm_C represents the molar mass of carbon (12.01 g/mol), and m_{soil} is the amount of soil in each condition (0.025 kg).

2.5.2. Nitrogen mineralization test

This test was also based on the AFNOR FD U44-163, (2018) standard. Biochar (25 tons/ha) and LD (170 tons/ha) were added and mixed with the soil as follows: soil, soil + biochar (B25), soil + LD + biochar (B25), and soil + LD. The experiment was carried out in soil cups (25 g of dry soil). Ammonium (NH_4^+) and nitrate (NO_3^-) ions were extracted from three repeats after 0, 7, 14, 28, 56, and 90 days of incubation at 28 °C with moisture maintenance (pF 2.8). For each sampling date, a procedure to extract the mineral nitrogen contained in the samples by mixing the soil with 100 mL of a KCl solution (1 mol/L) was carried out. The samples were placed on a rotating agitation device for 1 hour (Heidolph, Reax 20, Germany). The samples were then filtered using filter paper. The filtrate samples were frozen before being sent to the laboratory for determination of the ammonia nitrogen levels as NH_4^+ and ammonium nitrate. The measurement of NH_4 was performed according to the modified NF U 42-125, (1985) standard, while the measurement of NO_3 was performed by colorimetry (Hood-Nowotny et al., 2010).

2.5.3. Ammonia nitrogen volatilization (NH_3)

The objective of this experiment was to estimate the loss of nitrogen by evaporation of ammonia nitrogen (NH_3) related to the supply of LD (170 kg N/ha), with or without biochar at 25 tons/ha (B25), using a closed dynamic flow system. The following conditions were investigated: soil, soil + biochar (B25), soil + LD + biochar (B25), and soil + LD. The altered soils were incubated for 15 days and added at 183 g. All of the conditions were repeated four times. To allow microbiological activity in each enclosure, distilled water was added to reach 60% of the soil retention capacity. Volatile ammonia nitrogen was captured in an acid trap. The traps were changed eight times over the 15-day period to determine the kinetics of the volatilization. The experimental system comprised three main parts: an incoming air condition control system (consisting of a bottle of distilled water, a bottle of sulfuric acid, and a second

bottle of distilled water); a 500 mL closed volatile chamber containing the modified soil (biochar with or without LD); and an acidic ammonia trapping system. The airflow was set to 600 L/h (1.25 L/min) at the chamber outlet. For each device, 9 samples were taken during this test, at 1, 2, 3, 6, 8, 10, 13, and 15 days. The acid trap (0.05 mol/L sulfuric acid) provides the protons needed to switch from gaseous NH_3 to NH_4^+. The acid traps were assayed by colorimetry to obtain the concentration of NH_4^+ in the volume of acid, thereby allowing determination of the amount of NH_3 that had evaporated. These amounts were related to the dry soil mass. The quantities were accumulated to determine the kinetics of the ammonia nitrogen volatilization.

2.5.4. Plant growth test

The agronomic value of coupling biochar (at doses of 25 and 50 tons/ha) with LD (170 kg N/ha) was evaluated by determining the growth parameters during the first vegetative stage (relative seed germination and aerial dry biomass) using tomato as the plant model. Plant experiments with tomato seeds were performed in small pots with a volume of 0.5 L placed in a growth chamber (Fitotron®, Weiss Gallenkamp, UK) according to the OECD 208 guidelines (2006) under controlled conditions. The environmental conditions during the testing were as follows: 16 h of light at 25 °C, 8 h of darkness at 18 °C, with 60% relative humidity for the periods of light and 80% relative humidity during the periods of darkness. Seven conditions were tested: soil alone; soil + industrial fertilizers using a mixture of DAP and ammonium nitrate to reach an application of 170 kg N/ha of mineral nitrogen and 10 kg P/ha of phosphorus (soil + IF); soil with LD applied at 170 kg N/ha (soil +LD); soil with LD and biochar application at 25 tons/ha (Soil + LD + B25); soil with LD and biochar application at 50 tons/ha (Soil + LD + B50); soil with biochar application at 25 tons/ha (soil + B25), and soil with biochar application at 50 tons/ha (soil + B50). The mixture for each condition was prepared at 70% of the water retention of soil. Six seeds were planted in each pot, using four

403 replicates for each condition. Each pot was manually sub-irrigated every 48 h by the addition
404 of water to reach the initial weight. After 70% germination of the control, two germinated
405 seeds were removed and four were kept for the growing period. After 41 days, the plants were
406 harvested by cutting them at ground level and they were then dried in an oven at 70 °C for 24
407 h. For each condition, the relative seed germination expressed as the percentage according to
408 Equation (9) and the aerial dry biomass expressed in (g DM/100 plants) was determined
409 according to Equation (10). Generally, a relative seed germination above 70% indicates low
410 phytotoxicity.

411 $$\text{Relative Seed Germination (\%)}$$
412 $$= (\text{Mean of germinated seed}/\text{Initial number of seeds}) \times 100 \qquad (9)$$

413 $$\text{Aerial dry biomass (g DM/ 100 plants)} = (\, M_{\text{dry (70 °C)}} /4) \times 100 \qquad (10)$$

414 where $M_{dry\,(70\,°C)}$ represents the mean of the aerial dry biomass (g DM) for each condition and
415 4 is the number of plants in each pot at harvesting time.

416 To compare the different conditions tested, the analysis of variance (ANOVA) method was
417 used to analyze the impact of the various fertilization modes, and the confidence level
418 considered was 95%.

419 ## 3. Results and Discussion

420 ### 3.1. Anaerobic digestion

421 In the first instance, anaerobic co-digestion of wastewater sludge and quinoa residues was
422 investigated in mesophilic CSTR anaerobic digesters. The main physicochemical properties of
423 the quinoa residues and the wastewater sludge are reported in **Table 1**. The quinoa residues
424 were composed of 24.6%DM of cellulose, 14.1 %DM of hemicelluloses, and 7.0 %DM of
425 lignin. The quinoa residues had a low nitrogen content of 0.21%DM and a high C/N ratio of
426 216. All of these values are in agreement with what has previously been reported for
427 lignocellulosic biomass in the literature (Monlau et al., 2013). By contrast, the wastewater

sludge had a higher nitrogen content of 7.0%DM and a lower C/N ratio of 5.8. Interestingly, co-digestion of quinoa residues and wastewater sludge in the AD process resulted in a C/N ratio of 13, which is more in agreement with the C/N ratios that have been reported to be optimal for the AD process, with values ranging from 15 to 30 (Morales-Polo et al., 2018; Van et al., 2020).

First of all, biochemical methane potential tests were carried out, and a value of 236 ± 2 NL CH_4/kg VS was determined for the wastewater sludge and 237 ± 2 NL CH_4/kg VS for the quinoa residues (data not shown). In this study, quinoa and wastewater sludge exhibited similar methane potentials and such values are in agreement with previous studies that investigated methane potential of lignocellulosic biomass (Monlau et al., 2012) and wastewater sludge (Elbeshbishy et al., 2012). Monlau et al. (2012) have reported methane potential ranging from 155 NL CH_4/kg TS to 300 NL CH_4/kg TS for various lignocellulosic biomasses. In parallel, co-digestion of quinoa residues and wastewater sludge (at 57.5/42.5% VS) resulted in a methane potential of 237 NL CH_4/kg VS demonstrating that the co-digestion did not exhibit positive synergy at BMP scale which has been previously reported in literature as the synergy effect depends on the biomass that are co-digested but also on the inoculum initially used (Elalami et al., 2019; Kim et al., 2019).

Then, co-digestion of quinoa residues and wastewater sludge was simulated for 16 weeks (corresponding to approximately three hydraulic retention times (HRTs) of 38 days) in mesophilic CSTR digesters, as shown in **Fig. 1A**. These durations are thought to be the minimum to assess the stability of the AD process (Sambusiti et al., 2013). After an increase of the organic loading rate during the two first weeks, the OLR was further set at 2 kg VS/m^3/day. During the overall period of the assay, the pH remained stable around 7.4 and the temperature was 38 ± 2 °C. All of the values presented below are averages of the values of the last HRTs (3^{rd} HRT).

453 The concentration of ammonium remained below 2.5 gN-NH_4/L, and no specific inhibition
454 was observed in terms of methane production. The threshold inhibition level for total
455 ammonia nitrogen reported in the literature varies from 1.5 to 2.5 g/L (Jiang et al., 2019;
456 Sambusiti et al., 2013; Yenigün and Demirel, 2013), but after inoculum acclimation
457 concentrations up to 2.5 g/L can be reach inside the anaerobic digester (Jiang et al., 2019).
458 The total ammonia nitrogen (TAN), which is generally defined as the sum of free ammonia
459 nitrogen (FAN, NH_3-N) and ammonium nitrogen (NH_4^+-N), is generated during the
460 hydrolysis of proteins, urea, and nucleic acids (Morozova et al., 2020). The content of VFAs
461 (data not shown) remained lower than 0.1 $g_{eq.acetate}$/L throughout the assay, thus demonstrating
462 good stability of the process and no acidification. These results were also reflected by the
463 FOS/TAC ratio (**Fig. 1B**), which was below the safety threshold value of 0.3 (Sambusiti et al.,
464 2013). To assess the performances and to identify the absence of inhibition, the average
465 specific methane yield was computed from the slope of the trend line fitting the data of the
466 cumulative methane production versus the cumulative VS fed to each reactor. As can be seen
467 in **Fig. 1C**, the final specific methane production was 238 NL CH_4/kg VS, corresponding to
468 100% of the result obtained by the biochemical methane potential (BMP) batch tests. These
469 observations are in agreement with previous studies that investigated the methane production
470 of organic wastes on a pilot scale (Sambusiti et al., 2013). In a previous study, Alagöz and
471 Yenigün, (2015) investigated mesophilic co-digestion of olive residue and waste activated
472 sludge, and they reported a methane potential of 210 NL CH_4/kg VS. Similarly, Li et al.
473 (2017) investigated mesophilic anaerobic co-digestion of waste activated sludge with tobacco
474 residues, and they reported a methane potential of 181 to 204 NL CH_4 /kg VS depending on
475 the substrate ratio. Finally, COD (chemical oxygen demand) balances were performed in
476 parallel on the overall AD system to monitor the absence of losses and closure of the organic
477 matter cycles. The balances are presented in **Fig. 2**. The COD recovery in the output (sum of

478 the COD of biogas, liquid and solid digestate) was equivalent to 95% of the COD of the input,
479 thus demonstrating that the matter fluxes are well evaluated and identified. At the end of the
480 3rd HRT, the digestate was separated into a liquid and a solid fraction by a wine press, and the
481 solid fraction was oven-dried. Pyrolysis of the solid digestate was investigated in the next
482 section.

483 **3.2. Pyrolysis**

484 Pyrolysis was carried out on the solid fraction of the digestate at 500 °C for 1 h after drying of
485 the solid digestate. The pyrolysis products distribution was as follows: 40 ± 1.2 wt% biochar,
486 35.8 ± 2.9 wt% bio-oil, and 23.7 ± 4.9 wt% syngas. The syngas produced during the pyrolysis
487 process was analyzed and the distribution of the syngas compounds is presented in **Fig.3**. The
488 LHV of the syngas was 11.8 MJ/Nm^3, which is in agreement with previously reported values
489 ranging from 12.9 MJ/Nm^3 to 15.7 MJ /N m^3 (Monlau et al., 2015b; Neumann et al., 2015;
490 Tayibi et al., 2021). The syngas mainly consisted of CO_2, CH_4, CO, and H_2, with a small
491 amount of C_2H_4, C_2H_6, and C_2H_2. The production of CO_2 and CO was mostly due to
492 decarboxylation and decarbonylation reactions (Jęczmionek and Porzycka-Semczuk, 2014).
493 The high content of CO_2 can also result from the cracking of remaining fibers such as
494 cellulose and hemicelluloses in the solid digestate fraction (Liu et al., 2011). In a recent study,
495 Ghysels et al. (2020) reported a similar composition of syngas from cocoa wastes after
496 pyrolysis at 500 °C. Indeed, on an N_2-free basis, the dominant compound in this stream was
497 carbon dioxide, at a concentration of 79.5 vol% for pyrolysis at 500 °C, and CO, CH_4, and H_2
498 were also present at concentrations of 13.2 vol%, 3.9 vol%, and 2.5 vol%, respectively.

499 In parallel to syngas, bio-oil was also generated during the pyrolysis process. At industrial
500 level, bio-oil separation by solvent seems to be a promising option with an organic phase that
501 can be used as a fuel or building blocks (Hossain et al., 2016; Pütün et al., 2005), whereas the
502 aqueous phase can be recirculated as feedstock for the AD process (Torri and Fabbri, 2014).

503 Hossain et al. (2016) have recently demonstrated the feasibility in an engine combustion of
504 using organic oil from solid digestate pyrolysis in blend with waste cooking oil and butanol.
505 In our study, the bio-oil obtained was separated into an organic and aqueous phase, at a ratio
506 of 23.1 wt%, and 76.9 wt%, respectively. Similarly, Ghysels et al. (2020) reported a ratio of
507 organic and aqueous phases of 25% and 75%, respectively, after pyrolysis of solid digestate
508 derived from cocoa wastes at 500 °C, which is in agreement with our study. The main
509 physicochemical properties of the organic phase of the bio-oil are summarized in **Table 2**.
510 The organic phase of the bio-oil had a high carbon content (70.5 wt%) and a low oxygen
511 content (14.9 wt%), which is required for bio-oil fuel applications. The higher heating value
512 (HHV) of the organic phase of the bio-oil (**Table 2)** was estimated to be 33.9 MJ/kg. This
513 HHV of bio-oil is higher than that reported by Opatokun et al. (2015) from food digestate
514 pyrolyzed at 500 °C with a calorific value of 13.5 MJ/kg, but in their case all the bio-oil was
515 considered and not only the organic phase. Nonetheless, our value was in the same range as
516 the value of 29.7 MJ/kg reported by Ghysels et al. (2020) after pyrolysis at 500 °C of solid
517 digestate from the anaerobic digestion of cocoa wastes. Generally, the organic phases from
518 bio-oil after pyrolysis of solid digestate at 500 °C have been reported to be dominated by
519 phenolic compounds (Ghysels et al., 2020; Tayibi et al., 2020a; Wei et al., 2018). For
520 instance, Wei et al. (2018) reported that the content of phenolic compounds was 70.4% in the
521 OP of the bio-oil produced from digestate (originating from sargassum anaerobic digestion)
522 pyrolyzed at 450 °C (Wei et al., 2018).

523 Finally, a third product was generated during the pyrolysis process (at 40 wt%), as a
524 carbonaceous material called biochar. Similarly, Opatokun et al. (2017) reported biochar
525 yields from 25 to 61%wt after pyrolysis at temperatures ranging from 300 °C to 700 °C of
526 solid digestate from anaerobic digestion of food wastes. Similarly, Neumann et al. (2015)
527 reported a biochar yield of 36%wt after pyrolysis at 500 °C of solid anaerobic digestate. The

528 produced biochar was characterized, and their main physicochemical properties are reported
529 in **Table 3** and compared to the EBC (European Biochar Certificate) and IBI (International
530 Biochar Initiative). The carbon content of the biochar was 47.2 wt%, indicating that it is a
531 class 2 biochar according to the IBI and that it is considered a bio carbon mineral (BCM) and
532 not a biochar according to the EBC (**Table 3**). Compared to the solid digestate, the amount of
533 O and H decreased in the biochar due to the decarboxylation and dehydration reactions during
534 the pyrolysis process. The ash content of the biochar was 38.2 wt% compared to only 15.9
535 wt% in the solid digestate (**Table 3)**. The relatively high ash content in the solid digestate can
536 be attributed to the fact that during the AD process the microorganisms convert the organic
537 fraction of the organics into CO_2 and CH_4 (Monlau et al., 2015a), resulting in a higher
538 concentration of inorganics in the digestate than in the original feedstocks. Macronutrients
539 (i.e., N, P, K, Mg, and Ca) were also analyzed in the solid digestate and the respective
540 biochar. Except for N, all the macronutrients were enriched in the biochar, which is in
541 agreement with previous publications that investigated biochar production from solid
542 digestate (Calamai et al., 2019; Monlau et al., 2016). Minor metals (*i.e.,* Pb, Cd, Cu, Ni, Hg,
543 Zn, Cr, and As) were also analyzed in the biochar. All of the values obtained were lower than
544 the maximal threshold levels recommended by the IBI (International Biochar Initiative).
545 Nonetheless, most of the values were higher than the threshold levels recommended by the
546 EBC (European Biochar Certificate), except for Hg, as shown in **Table 3**.

547 ### 3.3. Agronomic potential of coupling biochar and LD

548 #### 3.3.1. Plant growth tests on tomato plants

549 The impact of biochar (at 25 and 50 tons/ha) on the growth of tomatoes was investigated
550 during the first vegetative stage of the plants. The biochar concentration was chosen based on
551 the data in the literature (Glaser et al., 2015; Greenberg et al., 2019). Biochar has recently
552 been shown to be of considerable relevance to sustainable agriculture (Mandal et al., 2020;

553 Semida et al., 2019), even though biochar does not have any fertilizing actions and should
554 generally be added with a fertilizer (Greenberg et al., 2019; Ronga et al., 2020; Tayibi et al.,
555 2021). Since biochar does not provide an adequate supply of nutrients to serve as the sole
556 source of fertilization, combined effects with the LD (applied at 170 kg N/ha) were evaluated
557 on the relative seed germination and the aerial dry biomass of tomatoes. The liquid digestate
558 was composed of 3.8 wt% dry matter, 2.4 wt% volatile matter, 0.37 wt% total Kjeldahl
559 nitrogen (TKN), 0.15 wt% ammonium (NH_4^+), 0.27 wt% potassium (K_2O), and 0.25 wt%
560 phosphorus (P_2O_5).

561 Seed germination is a relevant indicator of potential phytotoxicity. LD added alone did not
562 affect the relative seed germination with 88 (±8) % in comparison to soil alone (92 (±9) %).
563 Interestingly, biochar addition at 25 and 50 tons/ha did not exhibit a negative impact on the
564 germination rate in comparison with soil alone and soil with industrial fertilizers, as shown in
565 **Fig. 4**. Indeed, relative seed germination of 92 (±9) %, 83 (±16) %, 79 (±8) % were reported
566 for soil alone, soil with 20 tons and 50 tons of biochar, respectively. Similarly, Bu et al.
567 (2020) investigated the effect of rice husk and woodchip biochar at various application rates
568 (1%, 2%, and 5% by weight) on seed germination of *Robinia pseudoacacia* in calcareous soil,
569 and they did not find that there was a negative impact (Bu et al., 2020). Furthermore, the
570 combination of LD and biochar did not exhibit a negative impact on germination in
571 comparison with soil alone and soil with industrial fertilizers. These results are also in
572 agreement with those of Tayibi et al. (2020a), who similarly did not observe a negative impact
573 on the germination of wheat when biochar (at 50 tons/ha) was added in combination with LD.

574 In parallel, the growth efficiency of tomato plants when the soil was amended by biochar (at
575 25 and 50 tons/ha) in combination with LD was also investigated during the first vegetative
576 growth stage (41 days). As shown in **Fig. 4,** all the conditions tested resulted in higher aerial
577 dry biomass production than the soil alone. More specifically, the application of LD increased

578 the aerial dry biomass to 18 gDM/100 plants compared to unamended soil (11.6 gDM/100
579 plants), although it was slightly lower than with industrial fertilizers (20.8 gDM/100 plants).
580 These results confirm the ability of LD to improve plant growth as previously demonstrated
581 (Elalami et al., 2020; Nkoa, 2014; Solé-Bundó et al., 2017). A higher aerial dry biomass was
582 obtained for the condition that combined biochar and LD, with an increase of 33% compared
583 to soil amended with biochar alone (ANOVA test: $p < 0.05$) and an increase of 88%
584 compared to soil only (ANOVA test: $p < 0.05$). In parallel, the dry biomass obtained for the
585 condition combining soil and LD was lower by 13.8% compared to the soil treated with
586 industrial fertilizers, although the results were not significantly different according to the
587 ANOVA test ($p = 0.18$)

588 Adding biochar with LD increased the dry biomass by 4.5% and 7.9% for 25 tons/ha and 50
589 tons/ha, respectively, compared to soil fertilized with industrial fertilizers, which shows the
590 positive effect of coupling biochar and LD.

591 Ronga et al. (2020) also assessed the effect of digestate and biochar fertilizers on the yield and
592 fruit quality of tomatoes grown in an organic farming system, and they obtained similar
593 results. Indeed, they demonstrated that plants fertilized with LD and biochar had the
594 maximum marketable yield (72 tons/ha), followed by BC (67 tons/ha), and LD (59 tons/ha);
595 while the lowest production (47 tons/ha) was recorded with unfertilized plants. These results
596 are in agreement with Glaser et al. (2015), who reported a positive effect on maize silage by
597 combining digestate with biochar. Glaser et al. (2015) demonstrated that the application of
598 biochar-digestate (at a biochar rate of 1 and 40 tons/ha and digestate at 200 kg N /ha) to maize
599 increased the yields and plant nutrition compared to pure digestate. Interestingly, at a
600 concentration of 40 tons/ha of biochar, the co-application of digestate with biochar
601 significantly increased the maize yield by 42% compared to untreated plants without biochar
602 addition (Glaser et al., 2015). Greenberg et al. (2019) also investigated the effect of coupling

603 LD with biochar added at 2 and 40 tons/ha on Zea mays. For both biochar applications, there
604 were no significant differences in terms of the rye above-ground biomass. Nonetheless, such
605 experiments must be extended in the future at a field-scale, and several parameters should be
606 carefully investigated such as the nature and the quantity of biochar, the digestate origin and
607 properties, the type of the soil, and climatic conditions.

608 **3.3.2. Ammonia volatilization, C and N mineralization**

609 In light of the results obtained with tomato plant growth during the first vegetative stage, the
610 effect of coupling LD with biochar at a dose of 25 tons/ha on other agronomic parameters
611 (*e.g.,* ammonia volatilization, C and N mineralization) was investigated. The addition of
612 biochar on the C mineralization compared with the control (soil alone) was investigated first,
613 as shown in **Fig. 5A**. A slight but non-significant reduction of C mineralization was observed
614 in the presence of biochar compared to the control (soil alone). Carbon dioxide is generally
615 released by microbial decay of residual organic matter (Semida et al., 2019). These results
616 confirm the capacity of biochar to sequester C in soils and to contribute to carbon
617 sequestration (Clough et al., 2013; Semida et al., 2019). Bruun and EL-Zehery, (2012)
618 investigated the effect of biochar addition to soil amended by barley straw. Without biochar,
619 48 ± 0.2% of the straw carbon was mineralized during the 451 days of the experiment. In
620 comparison, 45 ± 1.6% of C was mineralized after biochar addition at 1.5 g kg^{-1}. Similarly,
621 Yoo and Kang, (2012) demonstrated that the addition of biochar (at 2 wt%) in silt loam soils
622 did not affect the C mineralization compared with the soil alone. Fidel et al. (2019) also
623 investigated the impact of biochar (derived from wood) added at 0.5 wt%/wt% of silt soil on
624 CO_2 mineralization at different temperatures and humidity. They did not observe any
625 significant differences for any of the conditions between the CO_2 mineralization in the
626 biochar-amended soil and the unamended soil. The soil sequestration capacity of biochar
627 appears to depend on the soil typology, the climatic conditions, and the biochar origin

628 (Semida et al., 2019; Yoo and Kang, 2012). The addition of LD to the soil led to an
629 enhancement of the C mineralization due to the presence of soluble organic carbon that is
630 mineralized and NH_4^+, and the C mineralization rate was determined to be 1,517 mg C-
631 CO_2/kg dry soil. Finally, as shown in **Fig. 5A**, the combination of biochar and LD led to
632 equivalent C mineralization compared to soil amended with LD only, and a net C
633 mineralization of 1,539 mg C-CO_2/kg dry soil. Aside from potentially sequestering carbon,
634 the impact of biochar added alone or in combination with LD on the N dynamics by
635 performing N mineralization experiments was also investigated. The addition of biochar did
636 not appear to affect the N mineralization dynamics compared to soil alone, as shown in **Fig.**
637 **5B**. These results confirm that, aside from a high biochar C/N ratio of 17 that can further
638 increase the C/N of soil, no N immobilization was noted, thus suggesting that biochar is
639 composed of recalcitrant organic carbon (Semida et al., 2019). Furthermore, the absence of N
640 mineralization enhancement after biochar application can be explained by the biochar
641 capacity to absorb NH_4^+ and NO_3^- that masks N mineralization or by the low amount of
642 hydrolyzable organic N forms in biochar (Ameloot et al., 2015; Clough et al., 2013). The
643 same tendency was observed in the presence of LD, as shown in **Fig. 5B**, demonstrating that
644 the biochar did not affect the microbial population involved in N mineralization. The increase
645 in N mineralization was 129-135 mg $N_{mineral}$/kg dry soil.

646 The impact of coupling LD and biochar was also investigated in regard to ammonia
647 volatilization, as shown in **Fig. 5C**. Interestingly, the addition of biochar alone at 25 tons/ha
648 did not have any influence on the ammonia volatilization compared to soil alone. The addition
649 of digestate to the soil led to an increase of the ammonia volatilization of 1.8 mg N/kg dry soil
650 versus 0.4 mg N/kg dry soil for the non-amended soil. This increase of 1.8 mg N/kg dry soil
651 corresponded to 3.5% of the total nitrogen provided by the LD. This ammonia volatilization is
652 due to the presence of ammoniacal nitrogen present in the digestate that became volatilized

653 once applied in the soil (Nkoa, 2014; Plaimart et al., 2021). Similarly, Plaimart et al. (2021)
654 have reported that approximately 4.8% of the nitrogen was evaporated in the form of
655 ammonia after the application of digestate on a clay loam soil. Surprisingly, the co-application
656 of biochar and LD enhanced the ammonia volatilization by as much as 3 mg N/kg dry soil,
657 which can be explained by the fact that the alkaline nature of biochar added to soil promotes
658 ammonia volatilization (Sha et al., 2019). Such value of ammonia volatilization corresponded
659 to 5.8% of the total nitrogen initially provided and consequently biochar addition
660 simultaneously with LD resulted in 66% more N loss than LD application alone. Similar as
661 well as contradictory results have been observed in the literature, and the impact of biochar
662 addition on ammonia volatilization appears to depend on several parameters such as the
663 nature of the soil, the origin of the biochar, and the experimental conditions (Plaimart et al.,
664 2021; Sha et al., 2019).

665 **4. Conclusions**

666 In this study, an original cascading biorefinery approach that coupled AD and pyrolysis was
667 investigated for the valorization of organic wastes. AD led to a methane production of 219
668 NL CH_4/kg VS, and the organic phase (OP) of bio-oil and syngas from subsequent pyrolysis
669 of the solid digestate exhibited higher and lower heating values of 34 MJ/kg and 11.8
670 MJ/Nm^3, respectively. Specific attention was paid to combining biochar and anaerobic LD
671 for agronomic purposes. The characteristics of the biochar were in accordance with the IBI
672 recommendations for soil amendment. The co-application of biochar with LD significantly
673 increased the ammonia volatilization by 64% compared to LD application alone. Although
674 co-application of biochar with LD did not impact the C and N mineralization, their
675 simultaneous use improved the growth of tomato plants up to 25% compared to LD
676 application alone.

677 **Acknowledgments**

678 The authors wish to thank the Cherifian Office for Phosphates (OCP group) for funding the
679 ATLASS project.
680

681 **Table and Figure Captions:**

682 **Table 1.** The main chemical constituents of the feedstocks introduced into the anaerobic lab-
683 scale CSTR digester.

684 **Table 2.** The properties of the organic phase of bio-oil from the pyrolysis of the solid
685 digestate.

686 **Table 3.** The physicochemical properties of the solid digestate and the produced biochar
687 compared to the IBI (International Biochar Initiative) and the EBC (European Biochar
688 Certificate) recommendations.

689 **Fig.1.** (A) Organic loading rate effect, temperature, and pH changes during the AD process;
690 (B) Biomethane production and change in the NH_4^+ concentration during the AD; (C)
691 Cumulative biogas and methane production during the AD process vs. the cumulative VS
692 added.

693 **Fig.2**. Chemical oxygen demand (COD) mass balances of the AD CSTR process with quinoa
694 residues and wastewater sludge co-digestion.

695 **Fig.3**. Syngas distribution during the pyrolysis experimentation according to the temperature
696 process. Overall syngas composition produced during the pyrolysis process of solid digestate
697 are provided in the insert table.

698 **Fig.4**. Relative seed germination (%) and aerial dry biomass (gTS/100 plants) of tomato
699 plants.

700 **Fig.5**. (A) Microbial respiration, (B) Total nitrogen mineralization over time (from 0 to 91
701 days), and (C) Ammonia volatilization for the four conditions: soil, soil with biochar (at 25
702 tons/ha), soil with liquid digestate (LD), and soil with liquid digestate (LD) and biochar at 25
703 tons/ha (B25).

704

705

706 **Table 1.** The main chemical constituents of the feedstocks introduced into the anaerobic lab-
707 scale CSTR digester.

708

Parameter (units)	***Quinoa residues***	***Wastewater sludge***
DM (wt% FM)	90.1 ± 0.1	18.7 ± 0.1
VS (wt% DM)	88.9 ± 0.3	79.6 ± 2.2
C (wt%)	43.3 ± 0.2	41.2 ± 0.2
H (wt%)	6.0 ± 0.1	6.2 ± 0.2
N (wt%)	0.2 ± 0.0	7.0 ± 0.2
S (wt%)	0.1 ± 0.0	0.6 ± 0.0
O[a] (wt%)	40.5 ± 0.3	41.2 ± 0.5
Cellulose (wt%)	24.6 ± 0.4	-

Hemicelluloses (wt%)	14.1 ± 0.5	-
Klason lignin (wt%)	7.0 ± 0.3	-
Ash (wt%)	10.0 ± 0.2	3.8 ± 0.4

[a]***O%= 100%-C%-H%-N%-S%-Ash%***

Parameters (units)	Solid digestate	Biochar	IBI standards V2.0	EBC standards V4.8

709

710 **Table 2.** The properties of the organic phase of the bio-oil from pyrolysis of the solid
711 digestate.

712

713

Parameter (units)	Organic phase of bio-oil
C (wt%)	70.6 ± 0.9
H (wt%)	8.1 ± 0.7
N (wt%)	5.6 ± 0.5
S (wt%)	0.8 ± 0.1
O (wt%)[a]	14.9 ± 1.0
HHV (MJ/kg)	33.9
Density (kg/L)	1.1
[a] determined by difference	

714

715

716

717

718

719

720

721

722

723

724

725

726

727

728 **Table 3.** The physicochemical properties of the solid digestate and the produced biochar
729 compared to the IBI (International Biochar Initiative) and the EBC (European Biochar
730 Certificate) recommendations.

pH	7.7 ± 0.02	9.8 ± 0.06	-	-
C (wt%)	37.0 ± 2.0	47.2 ± 5.3	10 wt% Minimum •Class 1: ≥ 60wt% •Class 2: ≥ 30wt% and ≤ 60wt%. •Class 3: ≥ 10wt% and ≤ 30wt%.	Biochar ≥ 50wt% Bio Carbon Minerals (BMC) < 50wt%
H (wt%)	4.6 ± 0.4	1.6 ± 0.1	-	-
N (wt%)	2.8 ± 0.6	2.8 ± 0.2	-	-
S (wt%)	0.6 ± 0.1	0.4 ± 0.1	-	-
O[a] (wt%)	39.1 ± 1.7	9.7 ± 5.2	-	-
K (wt%)	1.3	3.1	-	-
P (wt%)	1.7	3.4	-	-
Mg (wt%)	0.4	0.6	-	-
Fe (wt%)	0.5	0.9	-	-
Ca (wt%)	1.7	3.6	-	-
Na (wt%)	0.2	0.4	-	-
H/C	0.13 ± 0.0	0.03 ± 0.0	-	-
O/C	1.06 ± 0.1	0.22 ± 0.13	-	-
Moisture (wt%)	8.3 ± 1.2	4.9 ± 1.3	-	-
Volatile matter (wt%)	60.4 ± 0.6	19.0 ± 0.7	Optional	Required
Fixed carbon (wt%)	15.8 ± 0.7	43.0 ± 0.0	-	-
Ash (wt%)	15.9 ± 1.2	38.2 ± 5.7	Required	Required
Cellulose (wt%)	17.8 ± 1.1	-	-	-
Hemicelluloses (wt%)	5.5 ± 0.0	-	-	-
Lignin (wt%)	18.3 ± 0.6	-	-	-
Minor metallic (mg/kg DM)				
Pb	28	54	70 - 500	< 150
Cd	2.8	5.2	1.4 - 39	< 1.5
Cu	220	389	63 - 1500	< 100
Ni	40	73	47 - 600	< 50
Hg	0.05	< 0.05	1 - 17	< 1
Zn	516	989	200 – 7000	< 400
Cr	120	209	64 – 1200	< 90
As	2.9	4.1	12 - 100	-

[a]***O% = 100%-C%-H%-N%-S%-Ash%***

731

732

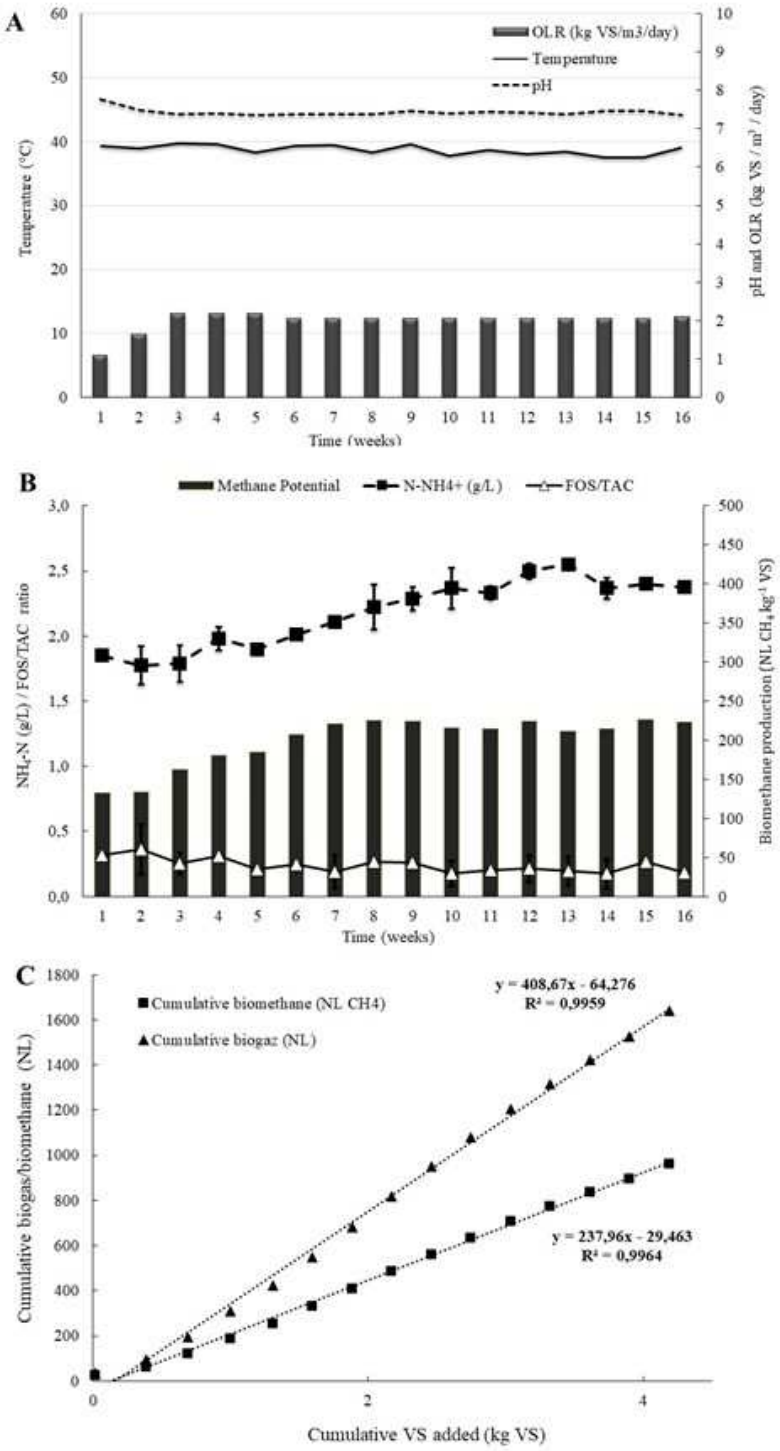

733

734 **Fig.1.** (A) Organic loading rate effect, temperature, and pH changes during the AD process;
735 (B) Biomethane production and change in the NH_4^+ concentration during the AD; (C)
736 Cumulative biogas and methane production during the AD process vs. the cumulative VS
737 added.

738

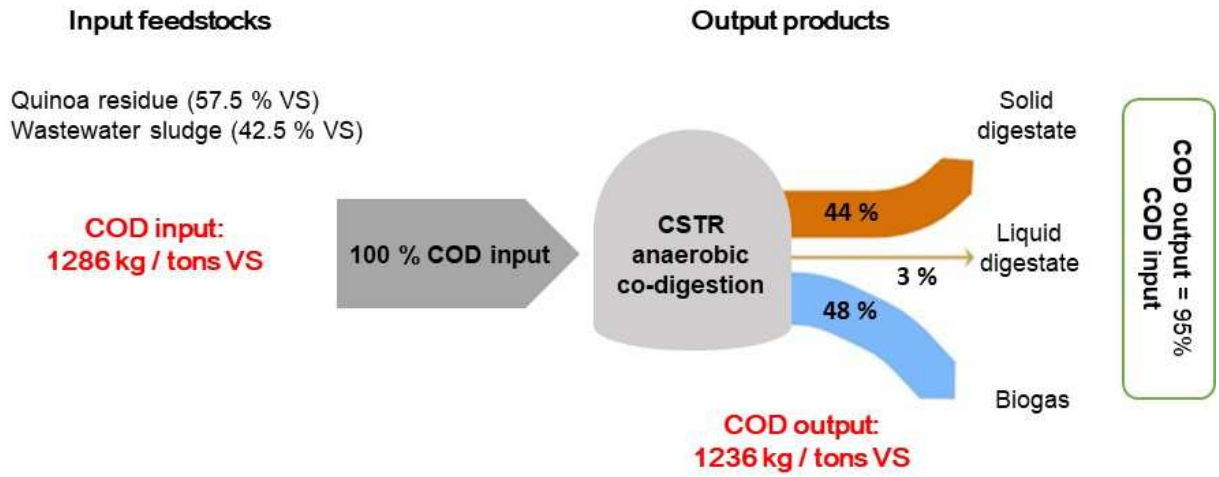

739

740 **Fig.2**. Chemical oxygen demand (COD) mass balances of the AD CSTR process with quinoa
741 residues and wastewater sludge co-digestion.

742

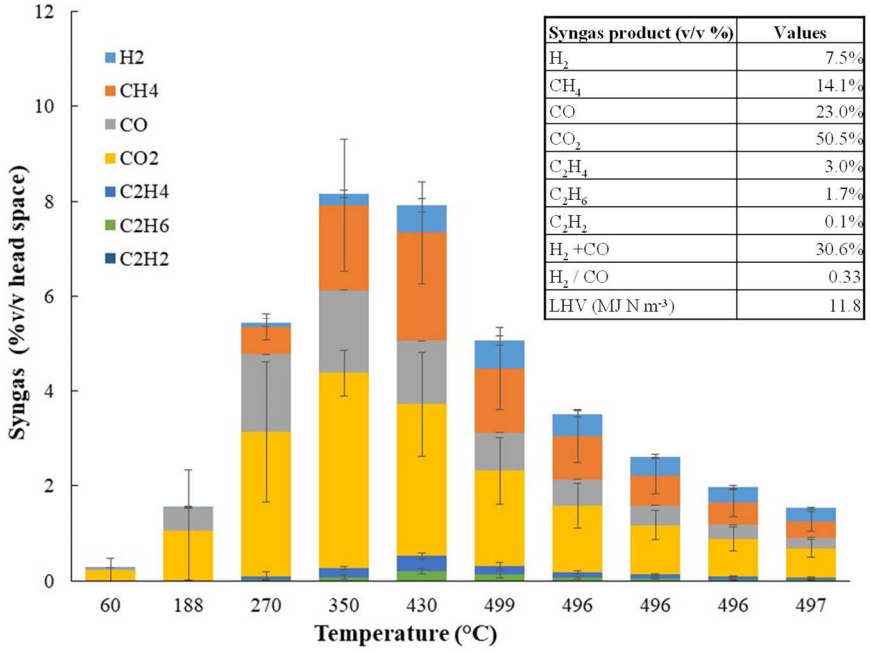

743

744

745 **Fig.3**. Syngas distribution during the pyrolysis experimentation according to the temperature
746 process. Overall syngas composition produced during the pyrolysis process of solid digestate
747 are provided in the insert table.

748

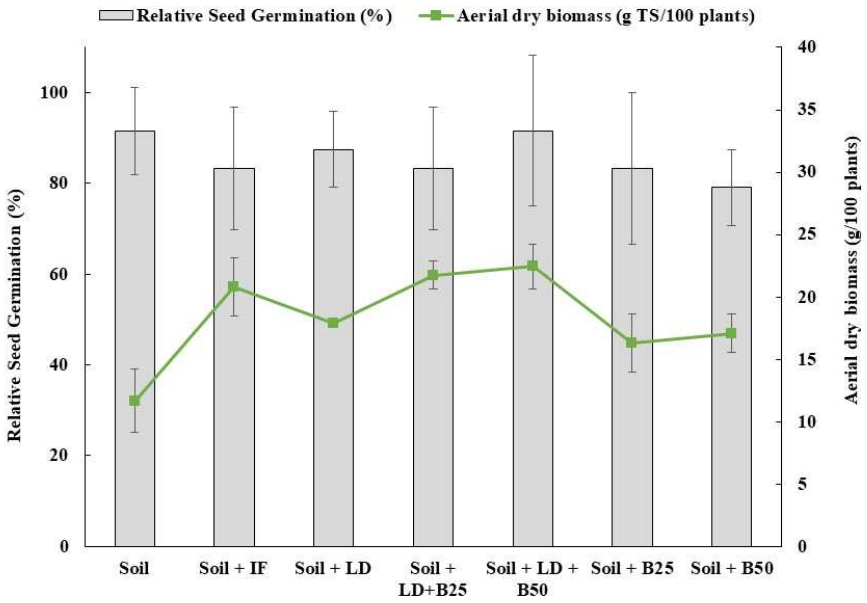

749

750 **Fig.4**. Relative seed germination (%) and aerial dry biomass (gDM/100 plants) of tomato
751 plants.

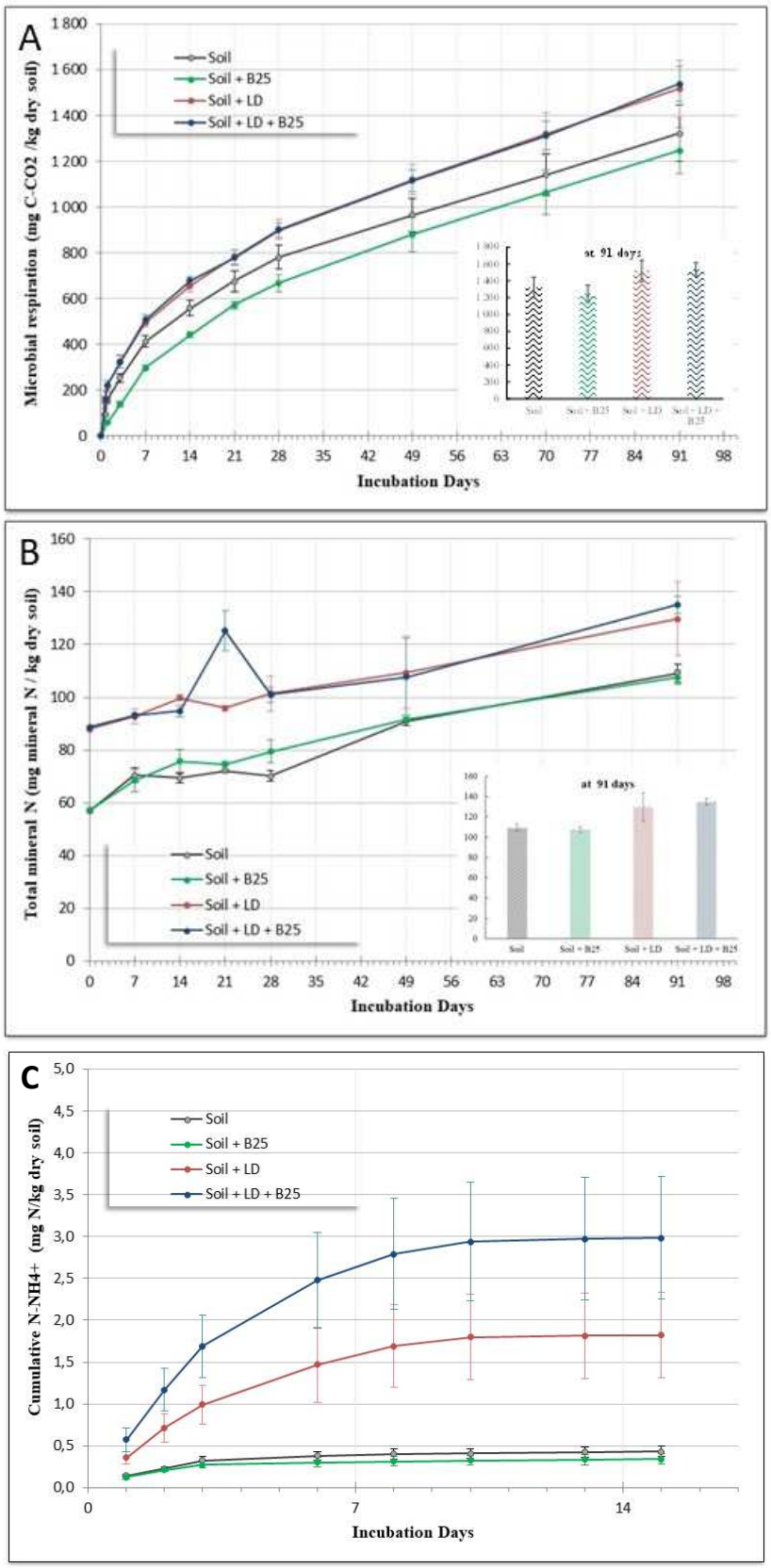

752 **Fig.5**. (A) Microbial respiration, (B) Total nitrogen mineralization over time (from 0 to 91
753 days), and (C) Ammonia volatilization for the four conditions: soil, soil with biochar
754 application at 25 tons/ha (soil + B25), soil with liquid digestate (soil + LD), and soil with
755 liquid digestate and biochar application at 25 tons/ha (soil + LD + B25).

References

1. Abdeljaoued, E., Brulé, M., Tayibi, S., Manolakos, D., Oukarroum, A., Monlau, F., Barakat, A., 2020. Bibliometric analysis of the evolution of biochar research trends and scientific production, Clean Technologies and Environmental Policy. Springer Berlin Heidelberg. https://doi.org/10.1007/s10098-020-01969-x

2. AFNOR FD U44-163, 2018. Organic amendments and growing media - Characterization of organic matter by the potential mineralization of carbon and nitrogen.

3. Akhiar, A., Battimelli, A., Torrijos, M., Carrere, H., 2017. Comprehensive characterization of the liquid fraction of digestates from full-scale anaerobic co-digestion. Waste Manag. 59, 118–128. https://doi.org/10.1016/j.wasman.2016.11.005

4. Alagöz, B.A., Yenigün, O., 2015. Enhancement of anaerobic digestion efficiency of wastewater sludge and olive waste : Synergistic effect of co-digestion and ultrasonic / microwave sludge pre-treatment. Waste Manag. 46, 182–188. https://doi.org/10.1016/j.wasman.2015.08.020

5. Alhamed, H., Biad, M., Saad, S., Masaki, M., 2018. Business Opportunities Report for Reuse of Wastewater in Morocco.

6. Ameloot, N., Sleutel, S., Das, K.C., KANAGARATNAM, J., NEVE, S. DE, 2015. Biochar amendment to soils with contrasting organic matter level : effects on N mineralization and biological soil properties. GCB Bioenergy 135–144. https://doi.org/10.1111/gcbb.12119

7. APHA, 2005. Standard methods for the examination of water and wastewater. Am. Public Heal. Assoc. 21st ed., 1220 p.

8. Barakat, A., Monlau, F., Solhy, A., Carrere, H., 2015. Mechanical dissociation and fragmentation of lignocellulosic biomass: Effect of initial moisture, biochemical and structural proprieties on energy requirement. Appl. Energy 142, 240–246. https://doi.org/10.1016/j.apenergy.2014.12.076

9. Belloulid, M.O., Hamdi, H., Mandi, L., Ouazzani, N., 2017. Solar drying of wastewater sludge: a case study in Marrakesh, Morocco. Environ. Technol. (United Kingdom) 40, 1316–1322. https://doi.org/10.1080/09593330.2017.1421713

10. Bruun, S., EL-Zehery, T., 2012. Biochar effect on the mineralization of soil organic matter. Pesqui. Agropecuária Bras. 47, 665–671. https://doi.org/10.1590/S0100-204X2012000500005

11. Bu, X., Xue, J., Wu, Y., Ma, W., 2020. Effect of Biochar on Seed Germination and Seedling Growth of Robinia pseudoacacia L . In Karst Calcareous Soils. Commun. Soil Sci. Plant Anal. 51, 352–363. https://doi.org/10.1080/00103624.2019.1709484

12. Calamai, A., Palchetti, E., Masoni, A., Marini, L., Chiaramonti, D., Dibari, C., Brilli, L., 2019. The Influence of Biochar and Solid Digestate on Rose-Scented Geranium (Pelargonium graveolens L'Hér.) Productivity and Essential Oil Quality. Agronomy 9, 260. https://doi.org/10.3390/agronomy9050260

13. Cazaudehore, G., Schraauwers, B., Peyrelasse, C., Lagnet, C., Monlau, F., 2019. Determination of chemical oxygen demand of agricultural wastes by combining acid hydrolysis and commercial COD kit analysis. J. Environ. Manage. 250, 109464. https://doi.org/10.1016/j.jenvman.2019.109464

14. Chandra, R., Takeuchi, H., Hasegawa, T., 2012. Methane production from lignocellulosic agricultural crop wastes : A review in context to second generation of biofuel production. Renew. Sustain. Energy Rev. 16, 1462–1476. https://doi.org/10.1016/j.rser.2011.11.035

15. Clough, T., Condron, L., Kammann, C., Müller, C., 2013. A Review of Biochar and Soil Nitrogen Dynamics. Agronomy 3, 275–293. https://doi.org/10.3390/agronomy3020275

16. Demichelis, F., Laghezza, M., Chiappero, M., Fiore, S., 2020. Technical , economic and environmental assessement of bioethanol biorefinery from waste biomass. J. Clean. Prod. 277, 124111. https://doi.org/10.1016/j.jclepro.2020.124111

17. Elalami, D., Carrere, H., Monlau, F., Abdelouahdi, K., Oukarroum, A., Barakat, A., 2019. Pretreatment and co-digestion of wastewater sludge for biogas production: Recent research advances and trends. Renew. Sustain. Energy Rev. 114, 109287. https://doi.org/10.1016/j.rser.2019.109287

18. Elalami, D., Monlau, F., Carrere, H., Abdelouahdi, K., Oukarroum, A., Zeroual, Y., Barakat, A., 2020. Effect of coupling alkaline pretreatment and sewage sludge co-digestion on methane production and fertilizer potential of digestate. Sci. Total Environ. 743, 140670. https://doi.org/10.1016/j.scitotenv.2020.140670

19. Elbeshbishy, E., Nakhla, G., Hafez, H., 2012. Biochemical methane potential (BMP) of food waste and primary sludge: Influence of inoculum pre-incubation and inoculum source. Bioresour. Technol. 110, 18–25. https://doi.org/10.1016/j.biortech.2012.01.025

20. Fabbri, D., Torri, C., 2016. Linking pyrolysis and anaerobic digestion (Py-AD) for the conversion of lignocellulosic biomass. Curr. Opin. Biotechnol. 38, 167–173. https://doi.org/10.1016/j.copbio.2016.02.004

21. Fernández, J.M., Nieto, M.A., López-de-Sá, E.G., Gascó, G., Méndez, A., Plaza, C., 2014. Carbon dioxide emissions from semi-arid soils amended with biochar alone or combined with mineral and organic fertilizers. Sci. Total Environ. 482–483, 1–7. https://doi.org/10.1016/j.scitotenv.2014.02.103

22. Fidel, R.B., Laird, D.A., Parkin, T.B., 2019. Effect of Biochar on Soil Greenhouse Gas Emissions at the Laboratory and Effect of Biochar on Soil Greenhouse Gas Emissions at the Laboratory and Field Scales. Soil Syst. https://doi.org/10.3390/soilsystems3010008

23. Ghysels, S., Acosta, N., Estrada, A., Pala, M., Vrieze, J. De, Ronsse, F., Rabaey, K., 2020. Integrating anaerobic digestion and slow pyrolysis improves the product portfolio of a cocoa waste biorefinery. Sustain. Energy Fuels 4, 3712–3725. https://doi.org/10.1039/d0se00689k

24. Giuliano, A., Bolzonella, D., Pavan, P., Cavinato, C., Cecchi, F., 2013. Co-digestion of livestock effluents, energy crops and agro-waste: Feeding and process optimization in mesophilic and thermophilic conditions. Bioresour. Technol. 128, 612–618. https://doi.org/10.1016/j.biortech.2012.11.002

25. Glaser, B., Wiedner, K., Seelig, S., Schmidt, H.P., Gerber, H., 2015. Biochar organic fertilizers from natural resources as substitute for mineral fertilizers. Agron. Sustain. Dev. 35, 667–678. https://doi.org/10.1007/s13593-014-0251-4

26. González-Arias, J., Fernández, C., Rosas, J.G., Bernal, M.P., Clemente, R., Sánchez, M.E., Gómez, X., 2019. Integrating Anaerobic Digestion of Pig Slurry and Thermal Valorisation of Biomass. Waste and Biomass Valorization 11, 6125–6137.

https://doi.org/10.1007/s12649-019-00873-w

27. González, R., González, J., Rosas, J.G., Smith, R., Gómez, X., 2020. Biochar and Energy Production : Valorizing Swine Manure through Coupling Co-Digestion and Pyrolysis. J. carbon Res. 6,43. https://doi.org/10.3390/c6020043

28. Greenberg, I., Kaiser, M., Gunina, A., Ledesma, P., Polifka, S., Wiedner, K., Mueller, C.W., Glaser, B., Ludwig, B., 2019. Substitution of mineral fertilizers with biogas digestate plus biochar increases physically stabilized soil carbon but not crop biomass in a field trial. Sci. Total Environ. 680, 181–189. https://doi.org/10.1016/j.scitotenv.2019.05.051

29. Hafner, S.D., Fruteau de Laclos, H., Koch, K., Holliger, C., 2020. Improving Inter-Laboratory Reproducibility in Measurement of Biochemical Methane Potential (BMP). Water 12, 1752. https://doi.org/10.3390/w12061752

30. Hood-Nowotny, R., Umana, N.H.-N., Inselbacher, E., Oswald- Lachouani, P., Wanek, W., 2010. Alternative Methods for Measuring Inorganic, Organic, and Total Dissolved Nitrogen in Soil. Soil Sci. Soc. Am. J. 74, 1018–1027. https://doi.org/10.2136/sssaj2009.0389

31. Hossain, A.K., Serrano, C., Brammer, J.B., Omran, A., Ahmed, F., Smith, D.I., Davies, P.A., 2016. Combustion of fuel blends containing digestate pyrolysis oil in a multi-cylinder compression ignition engine. Fuel 171, 18–28. https://doi.org/10.1016/j.fuel.2015.12.012

32. Im, S., Petersen, S.O., Lee, D., Kim, D.H., 2020. Effects of storage temperature on CH4 emissions from cattle manure and subsequent biogas production potential. Waste Manag. 101, 35–43. https://doi.org/10.1016/j.wasman.2019.09.036

33. Jęczmionek, Ł., Porzycka-Semczuk, K., 2014. Hydrodeoxygenation, decarboxylation and decarbonylation reactions while co-processing vegetable oils over a NiMo hydrotreatment catalyst. Part I: Thermal effects - Theoretical considerations. Fuel 131, 1–5. https://doi.org/10.1016/j.fuel.2014.04.055

34. Jiang, Y., Mcadam, E., Zhang, Y., Heaven, S., Banks, C., Longhurst, P., 2019. Ammonia inhibition and toxicity in anaerobic digestion : A critical review. J. Water Process Eng. 32, 100899. https://doi.org/10.1016/j.jwpe.2019.100899

35. Kim, Jinsu, Baek, G., Kim, Jaai, Lee, C., 2019. Energy production from different organic wastes by anaerobic co-digestion: Maximizing methane yield versus maximizing synergistic effect. Renew. Energy 136, 683–690. https://doi.org/10.1016/j.renene.2019.01.046

36. Kjeldahl, J., 1883. A New Method for the Determination of Nitrogen in Organic Matter. Zeitschrift für Anal. Chemie 22, 366–382.

37. Li, X., Xu, X., Huang, S., Zhou, Y., Jia, H., 2017. An efficient method to improve the production of methane from anaerobic digestion of waste activated sludge. Water Sci. Technol. 76.8, 2075–2084. https://doi.org/10.2166/wst.2017.313

38. Liu, C., Huang, J., Huang, X., Li, H., Zhang, Z., 2011. Theoretical studies on formation mechanisms of CO and CO2in cellulose pyrolysis. Comput. Theor. Chem. 964, 207–212. https://doi.org/10.1016/j.comptc.2010.12.027

39. Lv, P.M., Xiong, Z.H., Chang, J., Wu, C.Z., Chen, Y., Zhu, J.X., 2004. An experimental

885 study on biomass air – steam gasification in a fluidized bed 95, 95–101.
886 https://doi.org/10.1016/j.biortech.2004.02.003

887 40. Mandal, S., Pu, S., Adhikari, S., Ma, H., Kim, D., 2020. Technology Progress and future
888 prospects in biochar composites : Application and reflection in the soil environment.
889 Crit. Rev. Environ. Sci. Technol. 0, 1–53.
890 https://doi.org/10.1080/10643389.2020.1713030

891 41. Monlau, F., Barakat, A., Trably, E., Dumas, C., Steyer, J.P., Carrère, H., 2013.
892 Lignocellulosic materials into biohydrogen and biomethane: Impact of structural features
893 and pretreatment. Crit. Rev. Environ. Sci. Technol. 43, 260–322.
894 https://doi.org/10.1080/10643389.2011.604258

895 42. Monlau, F., Francavilla, M., Sambusiti, C., Antoniou, N., Solhy, A., Libutti, A.,
896 Zabaniotou, A., Barakat, A., Monteleone, M., 2016. Toward a functional integration of
897 anaerobic digestion and pyrolysis for a sustainable resource management. Comparison
898 between solid-digestate and its derived pyrochar as soil amendment. Appl. Energy 169,
899 652–662. https://doi.org/10.1016/j.apenergy.2016.02.084

900 43. Monlau, F., Kaparaju, P., Trably, E., Steyer, J.P., Carrere, H., 2015a. Alkaline
901 pretreatment to enhance one-stage CH4and two-stage H2/CH4production from
902 sunflower stalks: Mass, energy and economical balances. Chem. Eng. J. 260, 377–385.
903 https://doi.org/10.1016/j.cej.2014.08.108

904 44. Monlau, F., Sambusiti, C., Antoniou, N., Barakat, A., Zabaniotou, A., 2015b. A new
905 concept for enhancing energy recovery from agricultural residues by coupling anaerobic
906 digestion and pyrolysis process. Appl. Energy 148, 32–38.
907 https://doi.org/10.1016/j.apenergy.2015.03.024

908 45. Monlau, F., Sambusiti, C., Barakat, A., Guo, X.M., Latrille, E., Trably, E., Steyer, J.P.,
909 Carrere, H., 2012. Predictive models of biohydrogen and biomethane production based
910 on the compositional and structural features of lignocellulosic materials. Environ. Sci.
911 Technol. 46, 12217–12225. https://doi.org/10.1021/es303132t

912 46. Monlau, F., Sambusiti, C., Ficara, E., Aboulkas, A., Barakat, A., Carrère, H., 2015c. New
913 opportunities for agricultural digestate valorization: Current situation and perspectives.
914 Energy Environ. Sci. 8, 2600–2621. https://doi.org/10.1039/c5ee01633a

915 47. Morales-polo, C., Cledera-Castro, M. del M., Soria, Y.M., 2018. applied sciences
916 Reviewing the Anaerobic Digestion of Food Waste : From Waste Generation and
917 Anaerobic Process to Its Perspectives. Appl. Sci. 8. https://doi.org/10.3390/app8101804

918 48. Morozova, I., Nikulina, N., Oechsner, H., Krümpel, J., Lemmer, A., 2020. Effects of
919 Increasing Nitrogen Content on Process Stability and Reactor Performance in Anaerobic
920 Digestion. energies 13. https://doi.org/10.3390/en13051139

921 49. Neumann, J., Binder, S., Apfelbacher, A., Gasson, J.R., Ramírez García, P., Hornung, A.,
922 2015. Production and characterization of a new quality pyrolysis oil, char and syngas
923 from digestate - Introducing the thermo-catalytic reforming process. J. Anal. Appl.
924 Pyrolysis 113, 137–142. https://doi.org/10.1016/j.jaap.2014.11.022

925 50. NF U 42-125, 1985. Fertilizers - Determination of ammoniacal nitrogen in the presence of
926 other substances releasing ammonia under the effect of sodium hydroxide - Titrimetric
927 method.

928 51. Nkoa, R., 2014. Agricultural benefits and environmental risks of soil fertilization with
929 anaerobic digestates: A review. Agron. Sustain. Dev. https://doi.org/10.1007/s13593-
930 013-0196-z

931 52. Opatokun, S.A., Strezov, V., Kan, T., 2015. Product based evaluation of pyrolysis of food
932 waste and its digestate. Energy 92, 349–354.
933 https://doi.org/10.1016/j.energy.2015.02.098

934 53. Opatokun, S.A., Yousef, L.F., Strezov, V., 2017. Agronomic assessment of pyrolysed
935 food waste digestate for sandy soil management. J. Environ. Manage. 187, 24–30.
936 https://doi.org/10.1016/j.jenvman.2016.11.030

937 54. Pecchi, M., Baratieri, M., 2019. Coupling anaerobic digestion with gasification, pyrolysis
938 or hydrothermal carbonization: A review. Renew. Sustain. Energy Rev. 105, 462–475.
939 https://doi.org/10.1016/j.rser.2019.02.003

940 55. Plaimart, J., Acharya, K., Mrozik, W., Davenport, R.J., Vinitnantharat, S., Werner, D.,
941 2021. Coconut husk biochar amendment enhances nutrient retention by suppressing
942 nitrification in agricultural soil following anaerobic digestate application. Environ.
943 Pollut. 268, 115684. https://doi.org/10.1016/j.envpol.2020.115684

944 56. Pütün, A.E., Uzun, B.B., Apaydin, E., Pütün, E., 2005. Bio-oil from olive oil industry
945 wastes: Pyrolysis of olive residue under different conditions. Fuel Process. Technol. 87,
946 25–32. https://doi.org/10.1016/j.fuproc.2005.04.003

947 57. Rodier, J., 1975. Analysis of water, In: Environmental chemical analysis. Marr IL, Cresser
948 MS (Eds). Int. Textb. Company. Chapman Hall New York.

949 58. Ronga, D., Caradonia, F., Parisi, M., Bezzi, G., Parisi, B., Allesina, G., Pedrazzi, S.,
950 Francia, E., 2020. Using digestate and biochar as fertilizers to improve processing
951 tomato production sustainability. Agronomy 10.
952 https://doi.org/10.3390/agronomy10010138

953 59. Roubaud, A., Favrat, D., 2005. Improving performances of a lean burn cogeneration
954 biogas engine equipped with combustion prechambers. Fuel 84, 2001–2007.
955 https://doi.org/10.1016/j.fuel.2004.02.023

956 60. Sambusiti, C., Ficara, E., Malpei, F., Steyer, J.P., Carrère, H., 2013. Benefit of sodium
957 hydroxide pretreatment of ensiled sorghum forage on the anaerobic reactor stability and
958 methane production. Bioresour. Technol. 144, 149–155.
959 https://doi.org/10.1016/j.biortech.2013.06.095

960 61. Sawatdeenarunat, C., Nguyen, D., Surendra, K.C., Shrestha, S., Rajendran, K., Oechsner,
961 H., Xie, L., Kumar, S., Khanal, S.K., 2016. Anaerobic biorefinery: Current status,
962 challenges, and opportunities. Bioresour. Technol. 215, 304–313.
963 https://doi.org/10.1016/j.biortech.2016.03.074

964 62. Semida, W.M., Beheiry, H.R., Mamoudou, S., Simpson, C.R., El-Mageed, T.A.A., Rady,
965 M.M., Nelson, S.D., 2019. Biochar implications for sustainable agriculture and
966 environment : A review. South African J. Bot. J. 127.
967 https://doi.org/10.1016/j.sajb.2019.11.015

968 63. Seyedi, S., Venkiteshwaran, K., Zitomer, D., 2019. Toxicity of various pyrolysis liquids
969 from biosolids on methane production yield. Front. Energy Res. 7, 1–12.
970 https://doi.org/10.3389/fenrg.2019.00005

64. Sha, Z., Li, Q., Lv, T., Misselbrook, T., Liu, X., 2019. Response of ammonia volatilization to biochar addition : A meta-analysis. Sci. Total Environ. 655, 1387–1396. https://doi.org/10.1016/j.scitotenv.2018.11.316

65. Sluiter, A., Hames, B., Ruiz, R., Scarlata, C., Sluiter, J., Templeton, D., and Crocker, D., 2008. Determination of Structural Carbohydrates and Lignin in Biomass: Laboratory Analytical Procedure (LAP). Tech. Rep. NREL/ TP -510 -42618 1–15. https://doi.org/NREL/TP-510-42618

66. Solé-Bundó, M., Cucina, M., Folch, M., Tàpias, J., Gigliotti, G., Garfí, M., Ferrer, I., 2017. Assessing the agricultural reuse of the digestate from microalgae anaerobic digestion and co-digestion with sewage sludge. Sci. Total Environ. 586, 1–9. https://doi.org/10.1016/j.scitotenv.2017.02.006

67. Tayibi, S., Monlau, F., Mariase, F., Cazaudehore, G., Fayoud, N.-E., Oukarroum, A., Zeroual, Y., Barakat, A., 2021. Coupling anaerobic digestion and pyrolysis processes for maximizing energy recovery and soil preservation according to the circular economy concept. J. Environ. Manage. https://doi.org/10.1016/j.jenvman.2020.111632

68. Tayibi, S., Monlau, F., Oukarroum, A., Zeroual, Y., 2020. One - pot activation and pyrolysis of Moroccan Gelidium sesquipedale red macroalgae residue : production of an efficient adsorbent biochar. Biochar. https://doi.org/10.1007/s42773-019-00033-2

69. Torri, C., Fabbri, D., 2014. Biochar enables anaerobic digestion of aqueous phase from intermediate pyrolysis of biomass. Bioresour. Technol. 172, 335–341. https://doi.org/10.1016/j.biortech.2014.09.021

70. Tripathi, M., Sahu, J.N., Ganesan, P., 2016. Effect of process parameters on production of biochar from biomass waste through pyrolysis: A review. Renew. Sustain. Energy Rev. 55, 467–481. https://doi.org/10.1016/j.rser.2015.10.122

71. Troy, S.M., Nolan, T., Leahy, J.J., Lawlor, P.G., Healy, M.G., Kwapinski, W., 2013. Effect of sawdust addition and composting of feedstock on renewable energy and biochar production from pyrolysis of anaerobically digested pig manure. Biomass and Bioenergy 49, 1–9. https://doi.org/10.1016/j.biombioe.2012.12.014

72. Van, D.P., Fujiwara, T., Tho, B.L., Toan, P.P.S., Minh, G.H., 2020. A review of anaerobic digestion systems for biodegradable waste : Configurations , operating parameters , and current trends. Environ. Eng. Res. 25, 1–17.

73. Wei, Y., Hong, J., Ji, W., 2018. Thermal characterization and pyrolysis of digestate for phenol production. Fuel 232, 141–146. https://doi.org/10.1016/j.fuel.2018.05.134

74. Wei, Z., Li, Y., Hou, Y., 2018. Quick estimation for pollution load contributions of aromatic organics in wastewater from pulp and paper industry. Nord. Pulp Pap. Res. J. 33, 568–572.

75. Yenigün, O., Demirel, B., 2013. Ammonia inhibition in anaerobic digestion : A review. Process Biochem. 48, 901–911. https://doi.org/10.1016/j.procbio.2013.04.012

76. Yoo, G., Kang, H., 2012. Effects of Biochar Addition on Greenhouse Gas Emissions and Microbial Responses in a Short-Term Laboratory Experiment. J. Environ. Qual. 41, 1193–1202. https://doi.org/10.2134/jeq2011.0157

77. Zhao, Z., Li, Y., Quan, X., Zhang, Y., 2018. Improving the co-digestion performance of waste activated sludge and wheat straw through ratio optimization and ferroferric oxide

supplementation. Bioresour. Technol. 267, 591–598. https://doi.org/10.1016/j.biortech.2018.07.052